Supporting Information

Fixed-charge Trimethyl Pyrilium Modification Enables Enhanced Top-down Mass Spectrometry Sequencing of Intact Protein Complexes

Daniel A. Polasky[†], Frederik Lermyte[♯], Michael Nshanian[‡], Frank Sobott[♯°+], Phillip C. Andrews[ǁ], Joseph A. Loo[‡,§], and Brandon T. Ruotolo[†*]

† Department of Chemistry, University of Michigan, 930 N. University Ave, Ann Arbor, MI 48109

‡ Department of Chemistry and Biochemistry, University of California Los Angeles, Los Angeles, CA 90095

ǁ Department of Biological Chemistry, University of Michigan, 1150 W. Medical Center Dr., Ann Arbor MI, 48109

§ Department of Biological Chemistry, David Geffen School of Medicine, and UCLA/DOE Institute for Genomics and Proteomics, University of California Los Angeles, Los Angeles, CA 90095

♯ Department of Chemistry, University of Antwerp, Groenenborgerlaan 171, 2020 Antwerp, Belgium

° The Astbury Centre for Structural Molecular Biology, University of Leeds, Leeds, LS2 9JT, UK

+ School of Molecular and Cellular Biology, University of Leeds, Leeds, LS2 9JT, UK

Corresponding Author:

bruotolo@umich.edu

Phone: +1-734-615-0198

Fax: +1 -734-615-0198

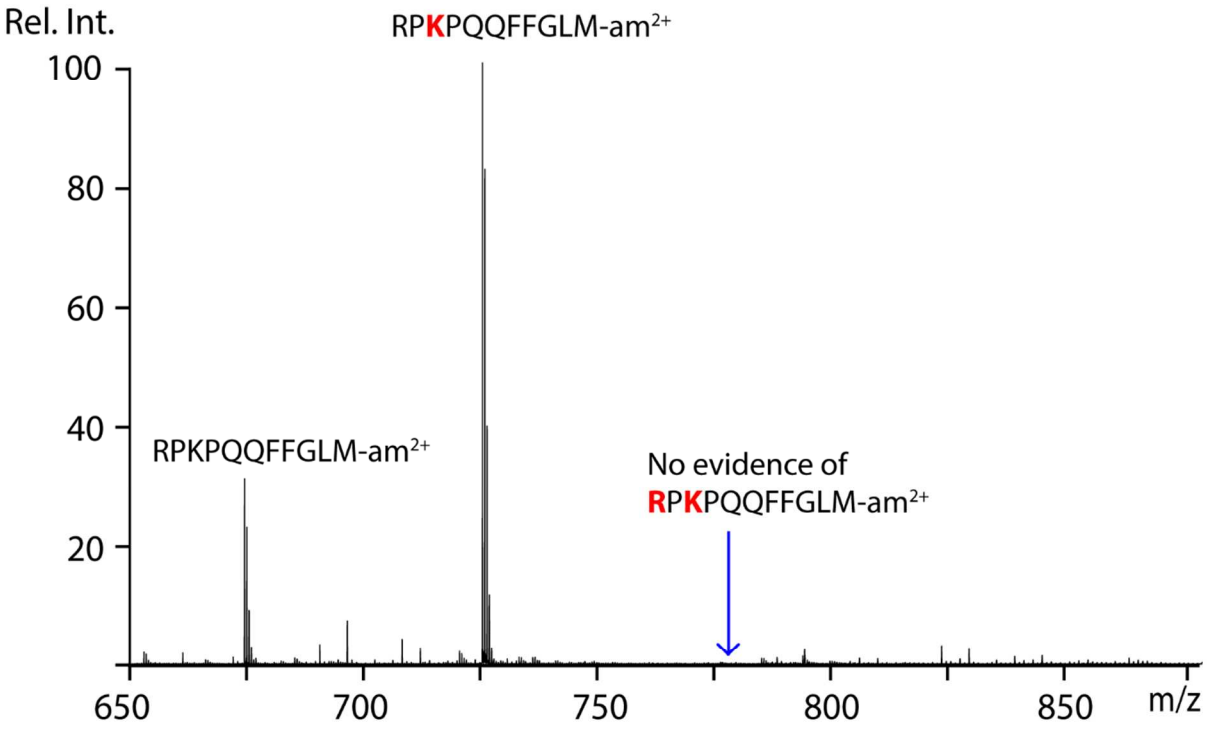

Figure S1: TMP modification of Substance P peptide (RPKPQQFFGLM-amide). Modification was performed under the same conditions as for proteins (see experimental), with TMP to Lysine molar ratio adjusted accordingly. The majority of the Substance P is modified at Lysine (red highlighted, center), but a significant minority remains unmodified after 24 hours. No evidence of modification at the n-terminal Arginine is observed, despite the availability of a primary amine at the terminus. No evidence of any other side reactions is observed.

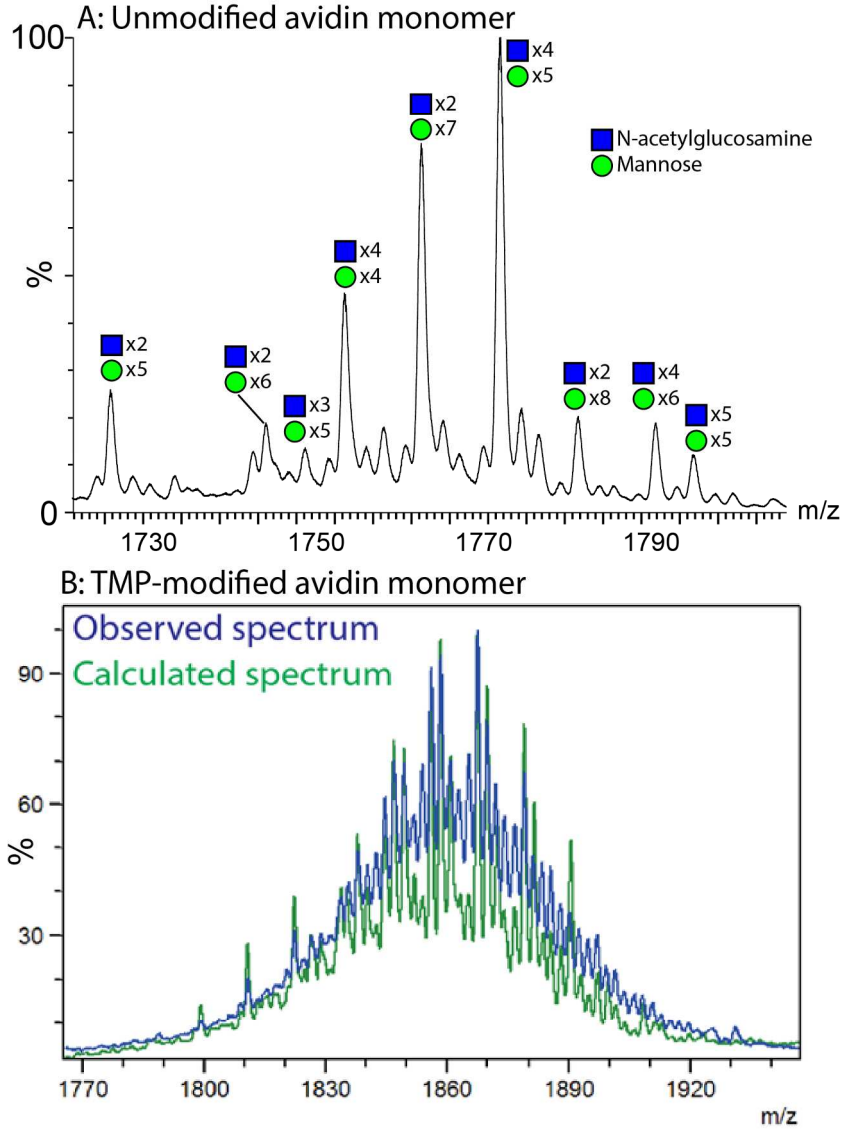

Figure S2: A) Mass spectrum of a monomer of unmodified avidin, displaying the heterogeneity of its glycosylation. This heterogeneity, combined with some variation in the number of TMP modifications observed on various monomers results in the spectrum shown in B. B) Modeled (calculated, green) and experimentally observed (blue) mass spectra for TMP-modified avidin monomer. The model was obtained by sequentially adding the *m/z* of a TMP modification to the spectrum of an unmodified avidin monomer to generated predicted spectra for each possible number of TMP modifications considered (0 to 15). A linear system of equations representing each possible modification state was solved for the optimal distribution of intensity (i.e. how much intensity in each modification state best recapitulates the observed mass spectrum) using the partial conjugate gradient method, resulting in the bar graph in Figure S2 and the calculated spectrum above. The major peaks in the observed spectrum are well represented in the calculated spectrum, though there is some discrepancy in the intensities. This is likely due to differences in peak width due to increased adduction in the TMP-modified data, a distinction which is not of great importance for this simple estimation of modification efficiency.

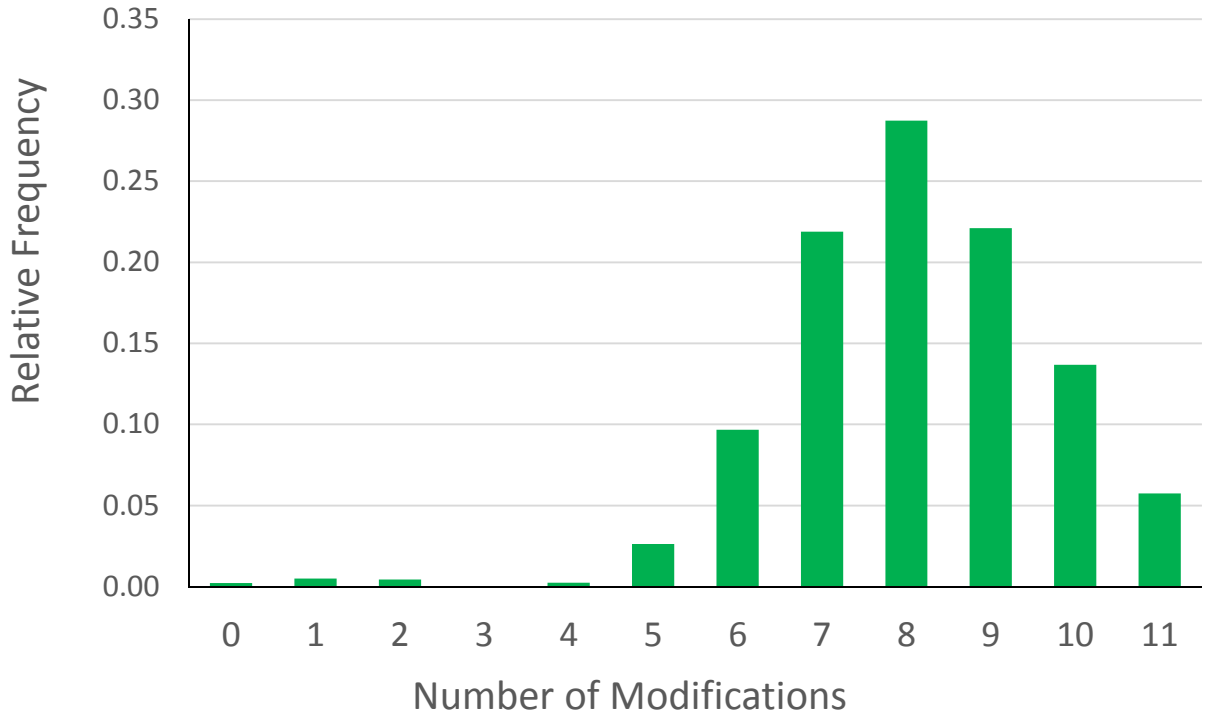

Figure S3: Number of TMP modifications to a single avidin monomer from model analysis described in Figure S1. There are 10 canonical sites (primary amines) available for modification in the form of nine lysine residues and the N-terminus, as well as at least one site on the glycosylated side chain of Asn-17 available for TMP modification. Data indicates generally good incorporation of the TMP tag with some variability in the final number of modifications. Achieving complete incorporation of tags is highly challenging in native, folded protein complexes as not all reaction sites are exposed to solvent, likely the primary cause of the distribution of modification states observed here. Aside from the glycan, no side reactions are observed with any non-Lysine amino acid residues.

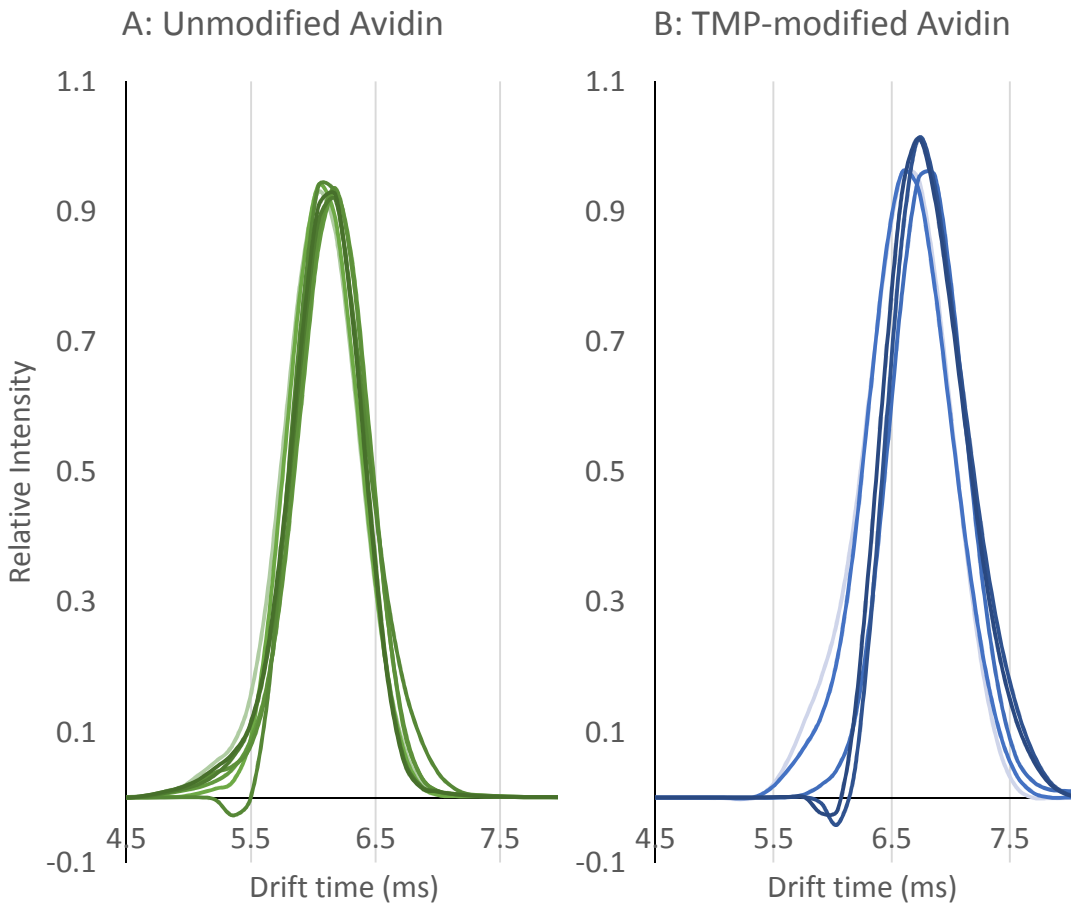

Figure S4: Ion mobility arrival time distributions of replicate analyses of the 17^{+} charge state of A) the unmodified (green lines, m/z 3750) and B) TMP-modified (blue lines, m/z 3960) avidin tetramer with no excess collisional activation energy. Both unmodified and TMP-modified distributions display a single peak, generally indicating the presence of a single, native-like global structure. The measured mass of unmodified Avidin tetramer was 63.9 kDa, while the measured mass of the TMP-modified Avidin was 67.5 kDa, with variation of approx. ±0.5 kDa between labeling reactions. The average centroid drift time for unmodified Avidin was 6.2 ms and the average for TMP-modified Avidin was 6.7 ms. The resulting 7% increase in drift time is in line with expectations from previous work in which Avidin was crosslinked with various reagents, resulting in 5-10% increases in CCS without perturbing structure[1]. We attribute the slight variations in drift time in TMP-modified Avidin to differences in final mass as a result of differences in labeling efficiency across several reaction trials.

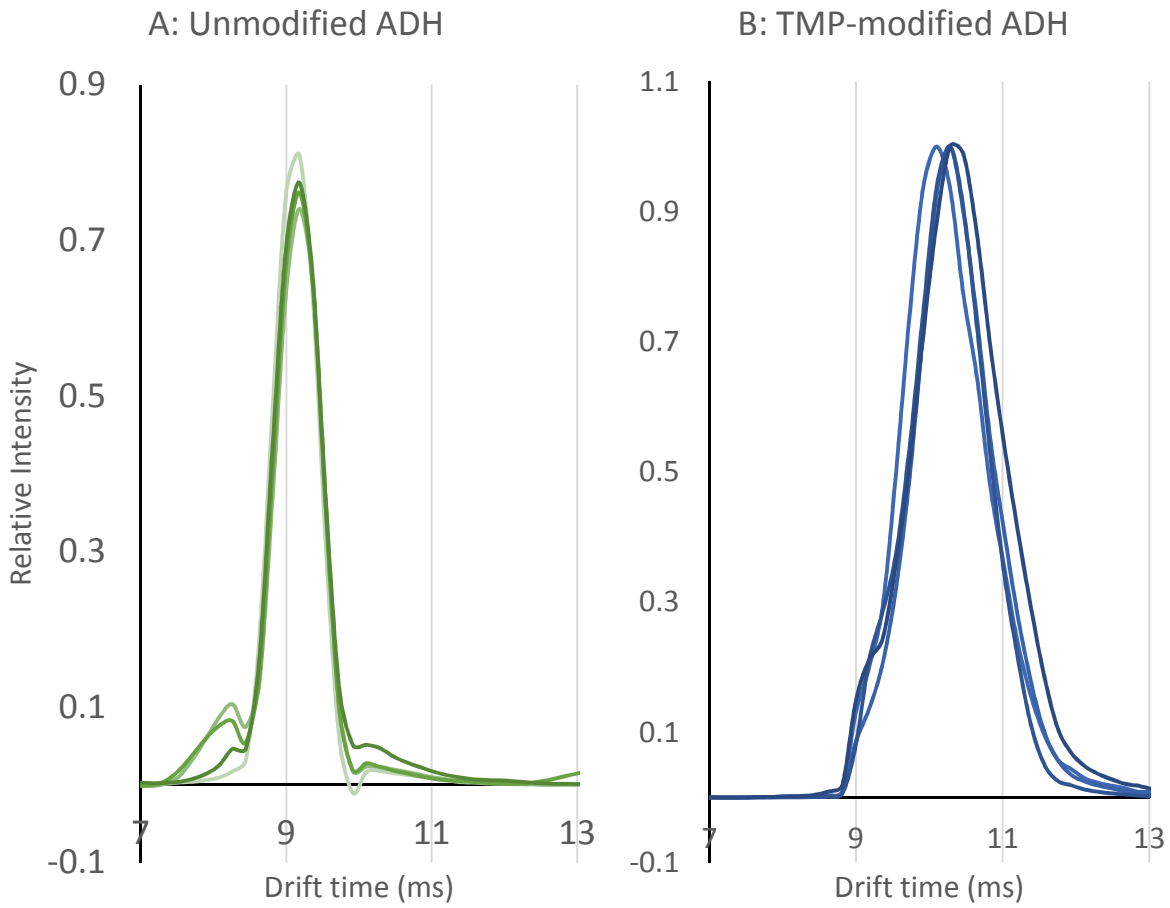

Figure S5: Ion mobility arrival time distributions of replicate analyses of the 26^{+} charge state of the A) unmodified (green lines, m/z 5675) and B) TMP-modified (blue lines, m/z 6100) ADH tetramer with no collisional activation energy applied. Both unmodified and TMP-modified distributions display a single peak, generally indicating the presence of a single, native-like global structure. The measured mass of unmodified ADH tetramer was 147.8 kDa, while the measured mass of the TMP-modified ADH was 158.3 kDa, with variation of approx. ±1 kDa between labeling reactions. The average centroid drift time for unmodified ADH was 9.2 ms and the average for TMP-modified ADH was 10.3 ms. The resulting 11% increase in drift time is in line with expectations from previous work in which several globular proteins were crosslinked with various reagents, resulting in 5-10% increases in CCS without perturbing structure[1]. We attribute the slight variations in centroid drift time and increased peak broadness in TMP-modified ADH to differences in final mass as a result of differences in labeling efficiency.

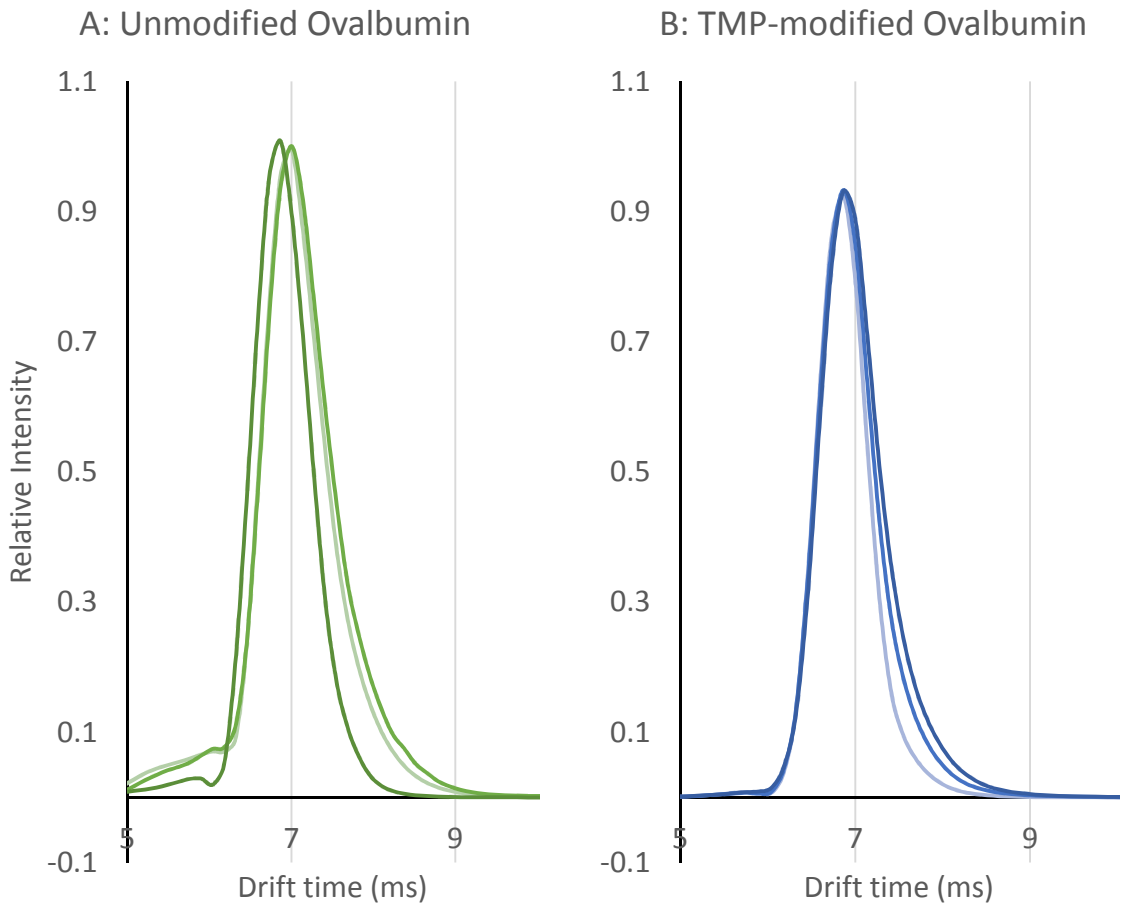

Figure S6: Ion mobility arrival time distributions of replicate analyses of the A) unmodified 12^+ (green lines, m/z 3720) and B) TMP-modified 13^+ (blue lines, m/z 3780) Ovalbumin monomer with no collisional activation energy applied. Note that different charge states were used for this analysis as the modified and unmodified charge state distributions were very narrow and did not share any high abundance peaks. Both unmodified and TMP-modified distributions display a single peak, generally indicating the presence of a single, native-like global structure. The measured mass of unmodified Ovalbumin monomer was 44.7 kDa, while the measured mass of the TMP-modified Ovalbumin monomer was 49.0 kDa, with variation of approx. ±0.5 kDa between labeling reactions. The average centroid drift time for unmodified Ovalbumin was 6.9 ms and the average for TMP-modified Ovalbumin was 6.9 ms. As the TMP-modified Ovalbumin here is at a higher charge state than the unmodified, it will have a larger collision cross section value despite the similarity in drift time, but, as in the case of ADH and Avidin, the increase in cross section is on par with the 5-10% observed following labeling of protein complexes in previous work[1].

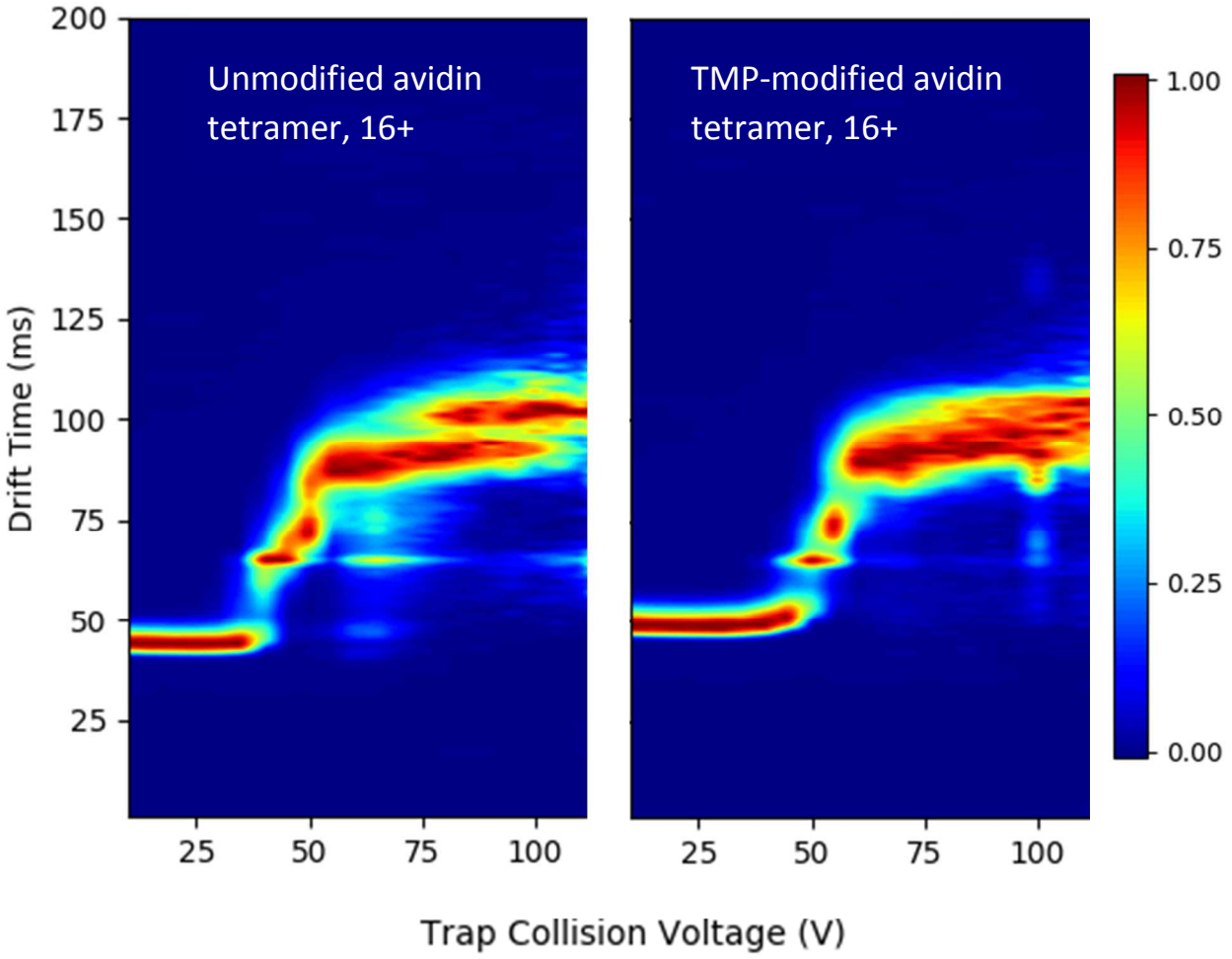

Figure S7: Collision induced unfolding (CIU) profiles of the same charge state of unmodified (left) and TMP-modified (right) avidin tetramer. The profiles show the increases in drift time (unfolding) as a function of applied collisional energy (trap collision voltage, x-axis). Notably, both modified and unmodified profiles show the same five features, albeit at slightly different intensities and onset voltages. This broad similarity is indicative of similar global structure (with slight changes possible to local structure), as we would expect following chemical modification with TMP. The similarity of the CIU profiles observed, combined with the same initial drift times (Figures S4-S6), indicates that TMP modification does not cause measureable structural changes in the protein complexes analyzed in this work.

Table S1: Table of fragment identifications for unmodified Avidin. Output of a representative single analysis of unmodified Avidin is presented. Information for the detected feature, including m/z, peak intensity, and charge is shown along with the identified match, including sequence, ion type, and error in parts per million (ppm). Data presented in the main body of the paper contain at least three replicates similar to the data presented here. Mass accuracy of identified features is consistent across all sequencing data presented.

Observed *m/z*	**Intensity**	**z**	**Calculated *m/z***	**Error (ppm)**	**Sequence**	**Ion Type**	**Neutral Losses**
386.2049	915.7	1	386.2034	-4.0	QKE	y3	H2O loss
505.2602	3383.0	1	505.2617	3.0	TQKE	y4	
516.3020	2148.0	2	516.3014	-1.0	TRLRTQKE	y8	
644.7045	2104.0	3	644.7094	7.7	TRVGINIFTRLRTQKE	y16	
661.3629	3832.8	1	661.3628	-0.1	RTQKE	y5	
668.3883	5143.9	3	668.3885	0.3	ATRVGINIFTRLRTQKE	y17	
711.0826	3183.6	3	711.0868	6.0	KATRVGINIFTRLRTQKE	y18	
767.1068	1295.3	3	767.1097	3.8	WKATRVGINIFTRLRTQKE	y19	H2O loss
767.4377	7494.1	3	767.4377	0.0	WKATRVGINIFTRLRTQKE	y19	NH3 loss
773.1131	321826.4	3	773.1132	0.2	WKATRVGINIFTRLRTQKE	y19	
774.4467	7157.3	1	774.4468	0.2	LRTQKE	y6	
805.7860	3798.8	3	805.7800	-7.4	DWKATRVGINIFTRLRTQKE	y20	NH3 loss
837.9861	6951.2	2	837.9861	0.0	VGINIFTRLRTQKE	y14	
844.1247	2611.8	3	844.1223	-2.8	DDWKATRVGINIFTRLRTQKE	y21	NH3 loss
868.7997	1850.1	3	868.8050	6.1	GDDWKATRVGINIFTRLRTQKE	y22	
900.8284	2272.7	3	900.8242	-4.7	IGDDWKATRVGINIFTRLRTQKE	y23	NH3 loss
906.4998	40845.2	3	906.4997	-0.1	IGDDWKATRVGINIFTRLRTQKE	y23	
906.4998	49389.6	3	906.4997	-0.1	IGDDWKATRVGINIFTRLRTQKE	y23	
930.5480	1790.7	1	930.5479	-0.1	RLRTQKE	y7	
944.8361	1916.7	3	944.8420	6.2	DIGDDWKATRVGINIFTRLRTQKE	y24	
958.0516	2846.4	2	958.0472	-4.5	TRVGINIFTRLRTQKE	y16	NH3 loss
977.1882	1571.2	3	977.1808	-7.6	NDIGDDWKATRVGINIFTRLRTQKE	y25	NH3 loss
982.8569	2636.1	3	982.8563	-0.6	NDIGDDWKATRVGINIFTRLRTQKE	y25	
986.3420	1466.3	5	986.3353	-6.7	RNGKEVLKTMWLLRSSVNDIGDDWKATRVGINIF TRLRTQKE	y42	NH3 loss
989.7440	27286.3	5	989.7406	-3.4	RNGKEVLKTMWLLRSSVNDIGDDWKATRVGINIF TRLRTQKE	y42	
989.7447	28554.2	5	989.7406	-4.1	RNGKEVLKTMWLLRSSVNDIGDDWKATRVGINIF TRLRTQKE	y42	
993.5626	5144.9	2	993.5658	3.2	ATRVGINIFTRLRTQKE	y17	NH3 loss
1002.0782	4202.8	2	1002.0791	0.8	ATRVGINIFTRLRTQKE	y17	
1013.5881	1644.7	1	1013.5851	-3.0	TRLRTQKE	y8	H2O loss
1015.8834	1959.1	3	1015.8791	-4.2	VNDIGDDWKATRVGINIFTRLRTQKE	y26	
1044.8885	3857.5	3	1044.8898	1.3	SVNDIGDDWKATRVGINIFTRLRTQKE	y27	
1073.9016	9649.0	3	1073.9005	-1.0	SSVNDIGDDWKATRVGINIFTRLRTQKE	y28	

1090.8537	4197.4	4	1090.8482	-5.1	VLKTMWLLRSSVNDIGDDWKATRVGINIFTRLRTQKE	y37	
1120.2614	2062.0	3	1120.2587	-2.5	RSSVNDIGDDWKATRVGINIFTRLRTQKE	y29	NH3 loss
1123.1134	1757.5	4	1123.1089	-4.0	EVLKTMWLLRSSVNDIGDDWKATRVGINIFTRLRTQKE	y38	
1150.1649	1920.6	2	1150.1609	-3.4	WKATRVGINIFTRLRTQKE	y19	H2O loss
1150.6540	4931.7	2	1150.6529	-0.9	WKATRVGINIFTRLRTQKE	y19	NH3 loss
1157.9599	2122.6	3	1157.9534	-5.6	LRSSVNDIGDDWKATRVGINIFTRLRTQKE	y30	NH3 loss
1159.1652	64333.9	2	1159.1662	0.9	WKATRVGINIFTRLRTQKE	y19	
1199.6634	4080.4	2	1199.6531	-8.6	DWKATRVGINIFTRLRTQKE	y20	2xNH3 loss
1207.6766	4882.6	2	1207.6744	-1.8	DWKATRVGINIFTRLRTQKE	y20	H2O loss
1208.1707	16175.5	2	1208.1664	-3.5	DWKATRVGINIFTRLRTQKE	y20	NH3 loss
1216.6796	217740.0	2	1216.6797	0.1	DWKATRVGINIFTRLRTQKE	y20	
1236.9298	14185.5	4	1236.9240	-4.7	RNGKEVLKTMWLLRSSVNDIGDDWKATRVGINIFTRLRTQKE	y42	
1256.6686	2299.4	2	1256.6746	4.8	DDWKATRVGINIFTRLRTQKE	y21	H2O and NH3 loss
1265.1884	2495.2	2	1265.1879	-0.4	DDWKATRVGINIFTRLRTQKE	y21	H2O loss
1274.1971	3418.0	2	1274.1932	-3.1	DDWKATRVGINIFTRLRTQKE	y21	
1291.7488	4246.3	1	1291.7481	-0.5	IFTRLRTQKE	y10	
1302.7136	2367.3	2	1302.7039	-7.4	GDDWKATRVGINIFTRLRTQKE	y22	
1346.7073	5396.5	1	1346.6998	-5.6	ARKCSLTGKWTN	b12	
1350.2423	3258.9	2	1350.2406	-1.3	IGDDWKATRVGINIFTRLRTQKE	y23	H2O loss
1359.2452	26576.5	2	1359.2459	0.5	IGDDWKATRVGINIFTRLRTQKE	y23	
1388.7719	3584.0	1	1388.7645	-5.3	NIFTRLRTQKE	y11	NH3 loss
1407.7525	2390.4	2	1407.7541	1.1	DIGDDWKATRVGINIFTRLRTQKE	y24	H2O loss
1416.7602	9258.7	2	1416.7594	-0.6	DIGDDWKATRVGINIFTRLRTQKE	y24	
1461.7386	3698.7	1	1461.7267	-8.1	ARKCSLTGKWTND	b13	
1465.2794	1795.3	2	1465.2676	-8.1	NDIGDDWKATRVGINIFTRLRTQKE	y25	NH3 loss
1473.7716	1909.9	2	1473.7809	6.3	NDIGDDWKATRVGINIFTRLRTQKE	y25	

Table S2: Table of fragment identifications for TMP-modified Avidin. Output of a representative single analysis of TMP-modified Avidin is presented. Information for the detected feature, including m/z, peak intensity, and charge is shown along with the identified match, including sequence, ion type, error in parts per million (ppm), and any modifications. Modifications are not localized to a specific residue. Data presented in the main body of the paper contain at least three replicates similar to the data presented here. Mass accuracy of identified features is consistent across all sequencing data presented.

Observed *m/z*	**Intensity**	**Calculated *m/z***	**Error (ppm)**	**Charge**	**Sequence**	**Ion Type**	**Neutral Losses**	**Mods**
460.3018	72667	460.3036	4.0	1	ARK	b3		TMP
508.2749	10406	508.2771	4.4	1	QKE	y3		TMP
517.8132	1686	517.8092	-7.8	2	RLRTQKE	y7		TMP
518.2854	2459	518.2868	2.7	1	ARKCS	a5		
535.3173	166498	535.3179	1.0	1	ARKC	a4		TMP
591.3139	14384	591.3142	0.6	1	TQKE	y4	H_2O	TMP
609.3249	8865	609.3248	-0.1	1	TQKE	y4		TMP
614.3459	1301	614.3443	-2.7	1	ARKCSL	a6	NH_3	
622.3487	6825	622.3499	1.9	1	ARKCS	a5		TMP
631.3693	1016	631.3708	2.4	1	ARKCSL	a6		
735.4367	4197	735.4340	-3.7	1	ARKCSL	a6		TMP
746.9185	6847	746.9174	-1.3	2	NIFTRLRTQKE	y11	NH_3	TMP
755.4105	3471	755.4059	-6.0	2	ARKCSLTGKWTN	a12	NH_3	2xTMP
760.4168	902	760.4134	-4.4	1	ARKCSLT	b7		
763.4360	1190	763.4289	-9.3	1	ARKCSL	b6		TMP
765.4265	4232	765.4259	-0.8	1	RTQKE	y5		TMP
774.4469	1970	774.4468	-0.1	1	LRTQKE	y6		
777.9180	48777	777.9167	-1.7	2	ARKCSLTGKWTN	b12		2xTMP
793.9047	7941	793.9090	5.5	2	ARKCSLTGKWTNDLG	a15	NH_3	
802.1246	1965	802.1254	1.1	3	WKATRVGINIFTRLRTQKE	y19	NH_3	TMP
807.8018	20064	807.8009	-1.0	3	WKATRVGINIFTRLRTQKE	y19		TMP
817.4417	1342	817.4349	-8.4	1	ARKCSLTG	b8		
819.4500	1234	819.4551	6.3	1	ARKCSLT	a7	NH_3	TMP
835.4317	19710	835.4301	-1.9	2	ARKCSLTGKWTND	b13		2xTMP
836.8197	3934	836.8131	-7.8	3	WKATRVGINIFTRLRTQKE	y19	NH_3	2xTMP
840.4724	1645	840.4677	-5.5	3	DWKATRVGINIFTRLRTQKE	y20	NH_3	TMP
846.1473	7762	846.1433	-4.8	3	DWKATRVGINIFTRLRTQKE	y20		TMP
851.4229	4625	851.4225	-0.5	2	ARKCSLTGKWTNDLGS	b16	NH_3	
861.4760	854	861.4834	8.6	1	LRTQKE	y6	NH_3	TMP
869.1517	4076	869.1519	0.3	3	DWKATRVGINIFTRLRTQKE	y20	H_2O, NH_3	2xTMP
874.8286	2901	874.8275	-1.3	3	DWKATRVGINIFTRLRTQKE	y20	H_2O	2xTMP
875.1609	9160	875.1555	-6.2	3	DWKATRVGINIFTRLRTQKE	y20	NH_3	2xTMP
878.5096	4140	878.5100	0.4	1	LRTQKE	y6		TMP

880.8302	48654	880.8310	0.9	3	DWKATRVGINIFTRLRTQKE	y20		2xTMP
907.4876	1044	907.4943	7.3	3	DDWKATRVGINIFTRLRTQKE	y21	H_2O, NH_3	2xTMP
913.5007	3367	913.4978	-3.1	3	DDWKATRVGINIFTRLRTQKE	y21	NH_3	2xTMP
930.5448	1374	930.5479	3.4	1	RLRTQKE	y7		
941.1863	5826	941.1874	1.2	3	IGDDWKATRVGINIFTRLRTQKE	y23		TMP
969.8678	2059	969.8716	3.9	3	IGDDWKATRVGINIFTRLRTQKE	y23	H_2O	2xTMP
975.8727	17062	975.8751	2.5	3	IGDDWKATRVGINIFTRLRTQKE	y23		2xTMP
1002.5460	1328	1002.5384	-7.6	3	DIGDDWKATRVGINIFTRLRTQKE	y24	H_2O and NH_3	2xTMP
1008.2047	1151	1008.2139	9.1	3	DIGDDWKATRVGINIFTRLRTQKE	y24	H_2O	2xTMP
1013.5892	1055	1013.5851	-4.1	1	TRLRTQKE	y8	H_2O	
1014.2164	5243	1014.2175	1.0	3	DIGDDWKATRVGINIFTRLRTQKE	y24		2xTMP
1018.9571	1296	1018.9624	5.2	5	GKEVLKTMWLLRSSVNDIGDDWKATRVGINIFTRLRTQKE	y40		4xTMP
1034.6190	3209	1034.6111	-7.6	1	RLRTQKE	y7		TMP
1046.1869	1136	1046.1869	0.0	3	ARKCSLTGKWTNDLGSNMTIGAVNSRGEF	a29	H_2O, NH_3	TMP
1047.3660	1745	1047.3639	-2.0	5	DRNGKEVLKTMWLLRSSVNDIGDDWKATRVGINIFTRLRTQKE	y43	H_2O, NH_3	2xTMP
1048.5677	1386	1048.5764	8.3	5	RNGKEVLKTMWLLRSSVNDIGDDWKATRVGINIFTRLRTQKE	y42	H_2O	3xTMP
1072.9928	8004	1072.9912	-1.5	5	RNGKEVLKTMWLLRSSVNDIGDDWKATRVGINIFTRLRTQKE	y42		4xTMP
1085.2468	1009	1085.2546	7.2	3	VNDIGDDWKATRVGINIFTRLRTQKE	y26		2xTMP
1117.6497	1988	1117.6482	-1.3	1	TRLRTQKE	y8	H_2O	TMP
1143.2652	1200	1143.2759	9.3	3	SSVNDIGDDWKATRVGINIFTRLRTQKE	y28		2xTMP
1202.6781	3787	1202.6845	5.3	2	WKATRVGINIFTRLRTQKE	y19	NH3	TMP
1211.1932	16059	1211.1978	3.8	2	WKATRVGINIFTRLRTQKE	y19		TMP
1251.1917	14023	1251.1927	0.8	2	DWKATRVGINIFTRLRTQKE	y20	H_2O, NH_3	TMP
1258.6901	1158	1258.6831	-5.5	4	RNGKEVLKTMWLLRSSVNDIGDDWKATRVGINIFTRLRTQKE	y42	NH_3	TMP
1260.1994	24177	1260.1980	-1.1	2	DWKATRVGINIFTRLRTQKE	y20	NH_3	TMP
1263.2265	32408	1263.2294	2.3	2	WKATRVGINIFTRLRTQKE	y19		2xTMP
1268.7108	54856	1268.7113	0.4	2	DWKATRVGINIFTRLRTQKE	y20		TMP
1269.2047	2347	1269.1945	-8.0	4	GKEVLKTMWLLRSSVNDIGDDWKATRVGINIFTRLRTQKE	y40	NH_3	4xTMP
1273.4495	3581	1273.4511	1.3	4	GKEVLKTMWLLRSSVNDIGDDWKATRVGINIFTRLRTQKE	y40		4xTMP
1288.9575	1875	1288.9556	-1.5	4	RNGKEVLKTMWLLRSSVNDIGDDWKATRVGINIFTRLRTQKE	y42		2xTMP
1291.7547	1318	1291.7481	-5.1	1	IFTRLRTQKE	y10		
1293.1997	1055	1293.2026	2.2	4	NGKEVLKTMWLLRSSVNDIGDDWKATRVGINIFTRLRTQKE	y41	H_2O, NH_3	4xTMP

1301.9529	1328	1301.9619	6.9	4	NGKEVLKTMWLLRSSVNDIGDDWKATRVGINIFTRLRTQKE	y41		4xTMP
1303.2217	40609	1303.2243	1.9	2	DWKATRVGINIFTRLRTQKE	y20	H_2O, NH_3	2xTMP
1308.7085	3375	1308.7062	-1.8	2	DDWKATRVGINIFTRLRTQKE	y21	H_2O, NH_3	TMP
1310.7185	4032	1310.7147	-2.9	4	RNGKEVLKTMWLLRSSVNDIGDDWKATRVGINIFTRLRTQKE	y42	NH_3	3xTMP
1311.7354	14221	1311.7375	1.6	2	DWKATRVGINIFTRLRTQKE	y20	H_2O	2xTMP
1312.2320	48925	1312.2296	-1.9	2	DWKATRVGINIFTRLRTQKE	y20	NH_3	2xTMP
1314.9802	5520	1314.9713	-6.7	4	RNGKEVLKTMWLLRSSVNDIGDDWKATRVGINIFTRLRTQKE	y42		3xTMP
1317.7207	4651	1317.7115	-7.0	2	DDWKATRVGINIFTRLRTQKE	y21	NH_3	TMP
1320.7420	127863	1320.7428	0.6	2	DWKATRVGINIFTRLRTQKE	y20		2xTMP
1336.4779	2953	1336.4845	4.9	4	RNGKEVLKTMWLLRSSVNDIGDDWKATRVGINIFTRLRTQKE	y42	H_2O	4xTMP
1339.4632	1229	1339.4714	6.2	4	DRNGKEVLKTMWLLRSSVNDIGDDWKATRVGINIFTRLRTQKE	y43	NH_3	3xTMP
1356.7329	1000	1356.7346	1.3	4	FIDRNGKEVLKTMWLLRSSVNDIGDDWKATRVGINIFTRLRTQKE	y45		TMP
1365.4821	1021	1365.4872	3.8	4	DRNGKEVLKTMWLLRSSVNDIGDDWKATRVGINIFTRLRTQKE	y43	NH_3	4xTMP
1369.2467	3626	1369.2510	3.1	2	DDWKATRVGINIFTRLRTQKE	y21	H_2O	2xTMP
1378.2593	3582	1378.2563	-2.2	2	DDWKATRVGINIFTRLRTQKE	y21		2xTMP
1388.7740	3768	1388.7645	-6.8	1	NIFTRLRTQKE	y11	NH_3	
1395.8150	2525	1395.8112	-2.7	1	IFTRLRTQKE	y10		TMP
1411.2703	5956	1411.2775	5.1	2	IGDDWKATRVGINIFTRLRTQKE	y23		TMP
1454.2943	3369	1454.3038	6.5	2	IGDDWKATRVGINIFTRLRTQKE	y23	H_2O	2xTMP
1460.2875	4160	1460.2777	-6.7	2	DIGDDWKATRVGINIFTRLRTQKE	y24	NH_3	TMP
1463.3062	9844	1463.3091	1.9	2	IGDDWKATRVGINIFTRLRTQKE	y23		2xTMP
1468.7838	4196	1468.7910	4.9	2	DIGDDWKATRVGINIFTRLRTQKE	y24		TMP
1511.8054	6439	1511.8173	7.9	2	DIGDDWKATRVGINIFTRLRTQKE	y24	H_2O	2xTMP
1520.8195	12791	1520.8225	2.0	2	DIGDDWKATRVGINIFTRLRTQKE	y24		2xTMP
1554.8368	3229	1554.8261	-6.9	1	ARKCSLTGKWTN	b12		2xTMP
1565.8048	1389	1565.7899	-9.5	1	ARKCSLTGKWTND	b13		TMP

References:

(1) Samulak, B. M.; Niu, S.; Andrews, P. C.; Ruotolo, B. T. *Anal. Chem.* **2016**, *88*, 5290–5298.